SAND2018-10003R

Sandia National Laboratories
Albuquerque, New Mexico 87185

date: July 26, 2018

to: Distribution

from: Olivia McIntee, 1554

subject: Study of Anisotropic Elastic-Plastic Model Calibration

Abstract

The purpose of this study was to first assess the sensitivity of the parameters of elastic-plastic material models with anisotropic yield to choices in the calibration procedure. Two models were considered: Hill's 1948 and Barlat's Yld2004-18p. Subsequently, it was shown that calibration choices can have an effect on the values of the stress and strain at the ultimate point in uniaxial specimen responses. Finally, the calibrated Barlat model was able to reasonably reproduce the load-deflection and strain fields of a validation specimen that experienced multiaxial states of stress. Overall, it was found that the Barlat model resulted in a closer fit to the measurements and that the parameters of the calibration procedure should be varied to assess the sensitivity of the results.

1 Introduction

Previous research has been conducted at Sandia by Corona and Kramer (2017) on the calibration of elastic-plastic material models to account for the effects of yield anisotropy of metals. Calibration is a critical step in modeling the material response in engineering analysis. Through varying the parameters of the calibration procedures, uncertainty in model parameters can be assessed. There were two models used in this study: Hill (1948) and Yld2004-18p by Barlat et al (2005). The Hill model is quadratic with 6 anisotropy parameters while the Barlat model is non-quadratic with 18 anisotropy parameters and an exponent. Barlat's model is therefore more adept to model anisotropic material responses. The role of the calibration procedure is to determine the values of the model parameters.

This work utilizes the calibration prodcedure described in Figure 13 of Corona and Kramer (2017). Specifically, the flow stress weighting factor was varied while the weighting of the Lankford ratio was kept constant. This changed the values of the parameters of the models and therefore the material response, which is quantified by the flow stress and Lankford

ratio. The same material stock, an Al 7079 tubular extrusion, was used in this study as in Corona and Kramer (2017).

The calibration model results were compared to the experimental data used for calibration to calculate an error for the fit. Subsequently, this work assessed the effect of the choice of calibration parameters on the predicted responses of smooth uniaxial tension specimens. Finally, a single calibration fit for Barlat's model was used to simulate the responses of four tensile specimens, each cut in different orientations within the extrusion, with complex geometries that developed multiaxial stress states.

2 Results and Discussion

2.1 Calibration Sensitivity

Procedure

The weighting factor of the flow stress expression was incremented by 1 from 0 to 30, while the weight of the Lankford ratio was kept at unity.

Then the calibrated model parameters were used to determine the material response, such as the Lankford ratios and flow stresses, as determined by the flow rule. The results were then compared to the values measured in uniaxial tension specimens cut from 12 material orientations of the cylindrical extrusion. The specimens had a uniform square cross section as shown in Figures 3 and 4 in Corona and Kramer (2017).

Error in the flow stresses and Lankford ratios were calculated by

$$e_\sigma = \sum_{m=1}^{12} \left(\frac{f(\boldsymbol{\sigma}^m)}{Y} - 1 \right)^2 \tag{1}$$

and

$$e_r = \sum_{m=1}^{12} \left(\frac{r(\boldsymbol{\sigma}^m)}{r^m} - 1 \right)^2 \tag{2}$$

respectively, which sum the difference between the experimental values and output from the calibration model for the 12 orientations. Then the sum of e_σ and e_r gives the total error for each weight.

In (1) and (2) e_σ is the error in the flow stress, N_t is the number of calibrations, and $f(\boldsymbol{\sigma}^m)$ is the value of the yield function given by the measured yield stress of the m^{th} test. Y is a reference yield stress, taken to be the yield stress of the specimen aligned with the extrusion's axis. e_r is the error of the Lankford ratio. Similarly, $r(\boldsymbol{\sigma}^m)$ is the Lankford ratio calculated from the yield function and r^m is the Lankford ratio measured by the m^{th} test.

Results

The range of variation of the Hill parameters with the flow stress weighting factor are shown in Figures 1a and 1b. The same is shown for the Barlat parameters in Figures 2a-2g.

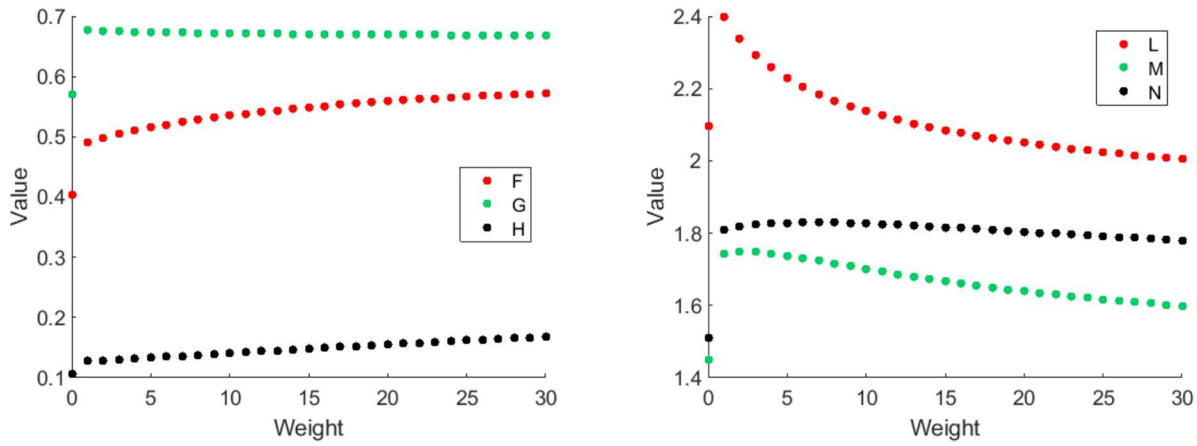

(a) (b)

Figure 1: Hill parameters vary with flow stress weighting factor. (a) Normal coefficients F, G, H and (b) shear coefficients L, M, N.

In Figure 1b the L parameter varied the most with weight, ranging from approximately 2.40 to 2.0. Figure 1a shows that the parameters G and H did not vary much with changes in weight, demonstrating how some parameters are not as sensitive to different calibrations. The parameters of the Barlat model have some variance, but as the weight increases the values tend to converge. Certain weights produced more variance than others. There was a large variance in the exponent value, and once again the value appeared to reach a steady state around 20 as weight increased. The change in the values of the model parameters caused the flow stresses and Lankford ratios to change as well. The Hill model results are shown in Figure 3 and the Barlat model results are shown in Figure 4. The index in these figures represents the 12 material orientations of the Al 7079 alloy specimens as described in Table 1. In Figures 3a and 4a, the blue circles represent that model calibration with the flow stress weighting factor, w_σ, set at 0 and the Lankford ratio weighting factor, w_r, kept at unity. This response makes sense because the value of the flow stress is not considered important in the calibration, so the model output will be the farthest from the measured value. Setting the weight at a value other than 0 will output results closer to the target flow stress values. Comparing the Hill and Barlat results show that Barlat stays closer to the target values than Hill.

Comparing the errors in the flow stress and Lankford ratios for Hill's model in Figures 5a and 5b, as the flow stress weight increases, the error of the flow stress, e_σ, decreases while the error of the Lankford ratio, e_r, increases. When the flow stress is considered more important, the Lankford ratio error is considered less important and dominates the total error trend as shown in Figure 5c.

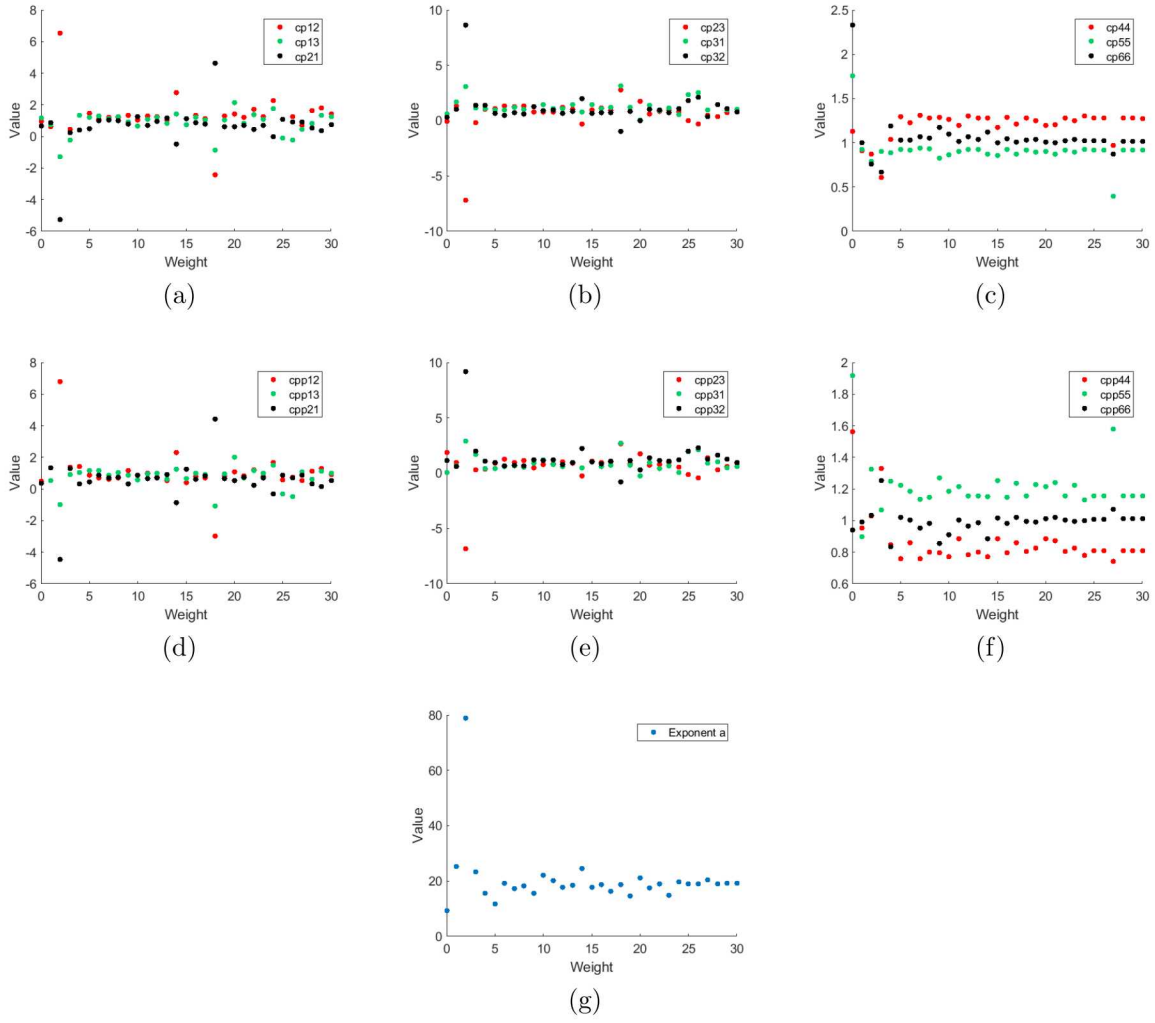

Figure 2: Barlat parameters vary with flow stress weighting factor. (a) $c'_{12}, c'_{13}, c'_{21}$ (b) $c'_{23}, c'_{31}, c'_{32}$ (c) $c'_{44}, c'_{55}, c'_{66}$ (d) $c''_{12}, c''_{13}, c''_{21}$ (e) $c''_{23}, c''_{31}, c''_{32}$ (f) $c''_{44}, c''_{55}, c''_{66}$ and (g) exponent a.

The errors in the Barlat model have a smaller range compared to the Hill model and show similar trends in Figures 6a-6c as the flow stress weighting factor increases. In Figures 6a-6c, the values output with $w_\sigma = 0$ were much higher than the other values, so they are not shown in the figures. These values can be found in Table 3. In Tables 2 and 3, the errors from two extreme cases are compared for the Hill and Barlat models repectively. In one case, $w_\sigma = 0$ and $w_r = 1$, showing what happens when the Lankford ratio value is the only calibration parameter considered important. Therefore, this case has the lowest error for the Lankford ratio and the highest error for the flow stress. When $w_\sigma = 1$ and $w_r = 0$, only the flow stress values were considered by the calibration procedure, so therefore the Lankford ratio and total errors were the highest of all the models. The error with respect to the Lankford ratio of the Barlat model was especially high for this case.

These results show why it is important to choose a weight wisely during the calibration

Table 1: Orientations of uniform cross section specimens.

Index	Orientation
1	$\theta = 0°$
2	$\theta = 15°$
3	$\theta = 30°$
4	$\theta = 45°$
5	$\theta = 60°$
6	$\theta = 75°$
7	$\theta = 90°$
8	$\phi = 45°$
9	$\phi = 60°$
10	$\phi = 90°$
11	$\psi = 45°$
12	$\psi = 60°$

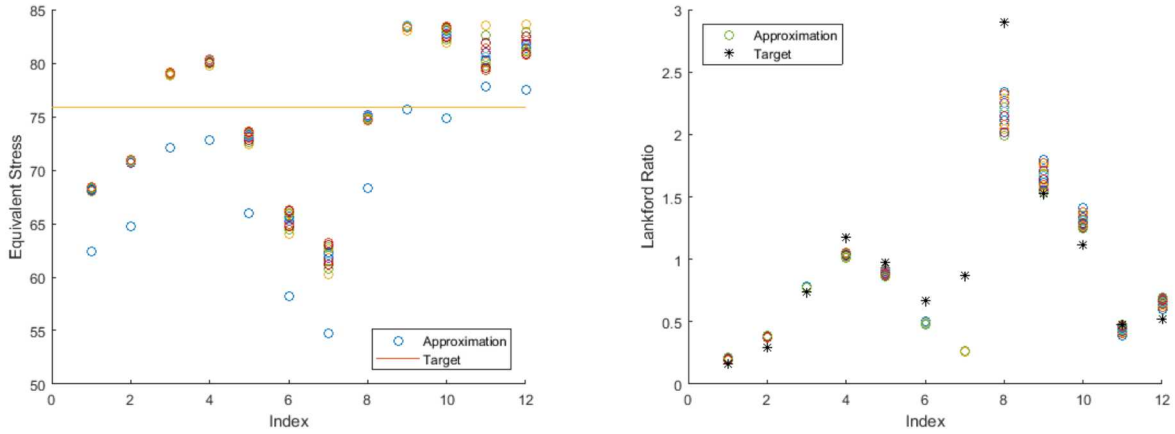

(a) (b)

Figure 3: The weighting factor affects the material response of the Hill model. (a) Flow stess and (b) Lankford ratios.

procedure. The weighting factor influences the material response of the model and therefore how closely the model fits the experimental data. If the model does not fit the data well, then it cannot be validated and used for analysis. Overall, it is recommended that these extreme cases are not chosen for analysis purposes, it is important when modeling anisotropic yield to include both the flow stresses and Lankford ratios in the calibration to more accurately depict the material response.

For the rest of this study, a weight of 10 was chosen for the flow stress weighting factor. This choice was made to match the previous study done by Corona and Kramer (2017) so that the results of the uniaxial tension test described in the forthcoming sections would

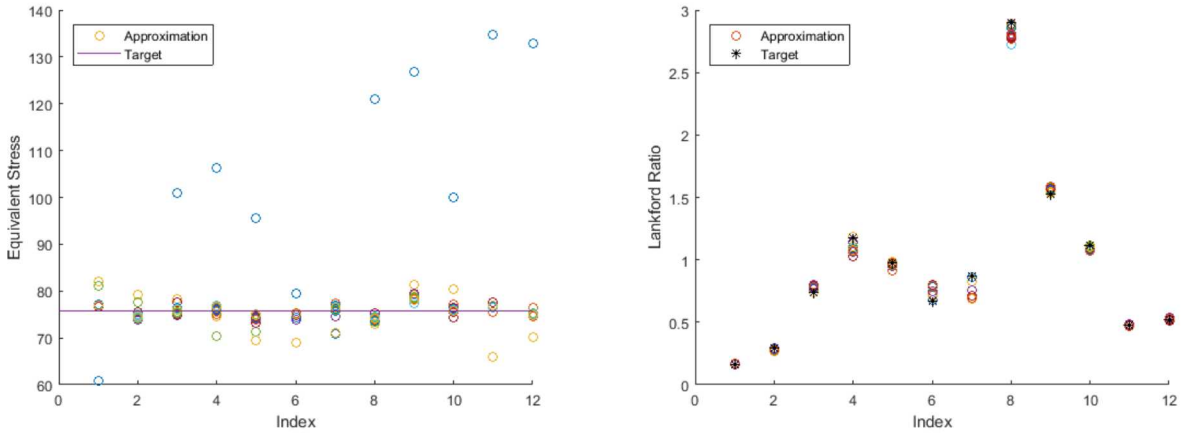

(a) (b)

Figure 4: The weighting factor affects the material response of the Barlat model. (a) Flow stess and (b) Lankford ratios.

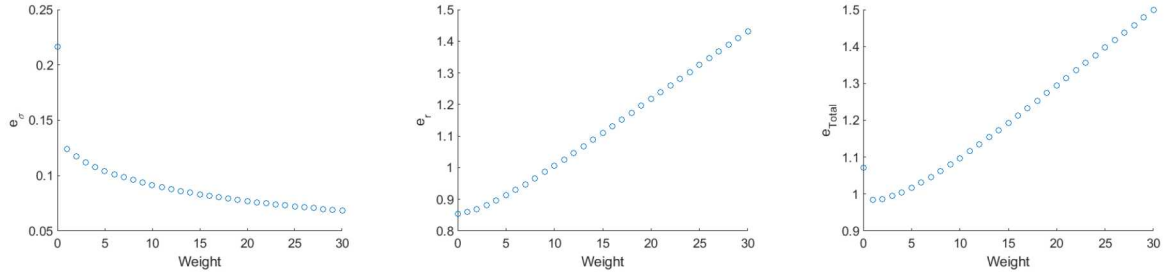

(a) (b) (c)

Figure 5: Errors of the Hill model depending on the flow stress weighting factor. (a) Error in flow stress (b) error in the Lankford ratios and (c) total error.

be comparable. However, based on the sensitivity calibration results in the current study, choosing a Lankford ratio weight of 1 and a flow stress weight of 5 may yield better results for the Barlat model. When w_σ= 5, the flow stress error is still decreasing, but the Lankford ratio error is still relatively low compared to greater weights. The Lankford ratio error has a large increase with the Barlat model in between weights 1 and 5. With weights less than 5, the flow stress error increases. It is shown in Figure 6 that after a weight of 5, the error appears to reach a steady state, so overall there is not a detrimental difference between choosing a weight of 10 or 5.

When using the Hill model, based on Figure 5, a weight range of 1-15 is recommended. Within this weight range the Lankford ratio error steadily increases as weight increases while the flow stress error steadily decreases. This is a subjective range and the analyst should judge which weight is best for his/her application.

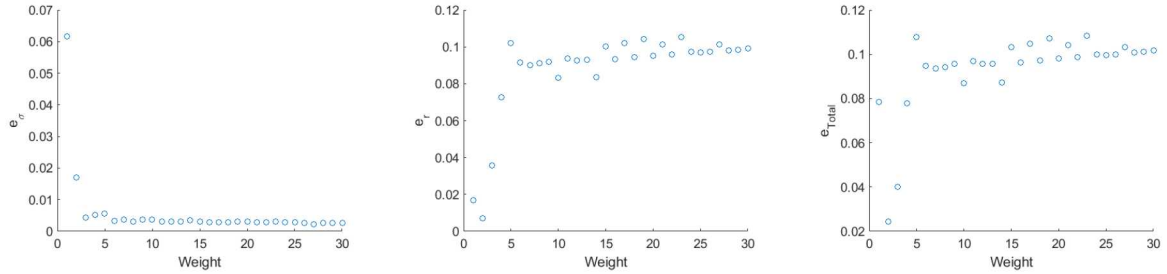

(a) (b) (c)

Figure 6: Errors of the Barlat model depending on the flow stress weighting factor. (a) Error in flow stress (b) error in the Lankford ratios and (c) total error.

Table 2: Comparison of errors for the Hill model for extreme values of w_σ, w_r.

Variable	$w_\sigma = 0$, $w_r = 1$	$w_\sigma = 1$, $w_r = 0$
Flow Stress Error	0.2167	0.0038
Lankford Ratio Error	0.8548	38.7251
Total Error	1.0715	38.7289

2.2 Uniform Cross Section, Uniaxial Tension Test Simulations

Procedure

Starting with a simple uniform cross section uniaxial tension geometry allowed for evaluation of the responses predicted by the Hill and Barlat models. Three of the 12 orientations previously studied by Corona and Kramer (2017) were chosen to be used in a uniaxial tensile test to demonstrate the effect of anisotropy: A0, A90, and B90 which are the axial, circumferential and through-thickness directions. The orientations of the material were modeled in Sierra/SM accordingly with a value of 10 chosen for the flow stress weighting factor. After running the simulations using Sierra/SM, the engineering stress-strain curves were compared to the corresponding experimental data. The values of the stress and strain at the ultimate point were calculated for selected flow stress calibration weights while keeping the Lankford ratio weight constant at unity. The stress and strain values were then normalized with the values corresponding with a flow stress weighting factor set at 10 in order to compare the results.

Table 3: Comparison of errors for the Barlat model for extreme values of w_σ, w_r.

Variable	$w_\sigma = 0$, $w_r = 1$	$w_\sigma = 1$, $w_r = 0$
Flow Stress Error	2.4614	$2.87E-23$
Lankford Ratio Error	0.0123	1039
Total Error	2.4737	1039

Results

The material responses modeled with Hill are shown in Figures 7a-7c. A0 was the orientation used for calibration of the hardening function, so as shown in Figure 7a, there is an insignificant difference between the model simulation and the experiment. There is some error in the plastic strain region that can be seen for A90 and B90 as shown in Figures 7b, and 7c.

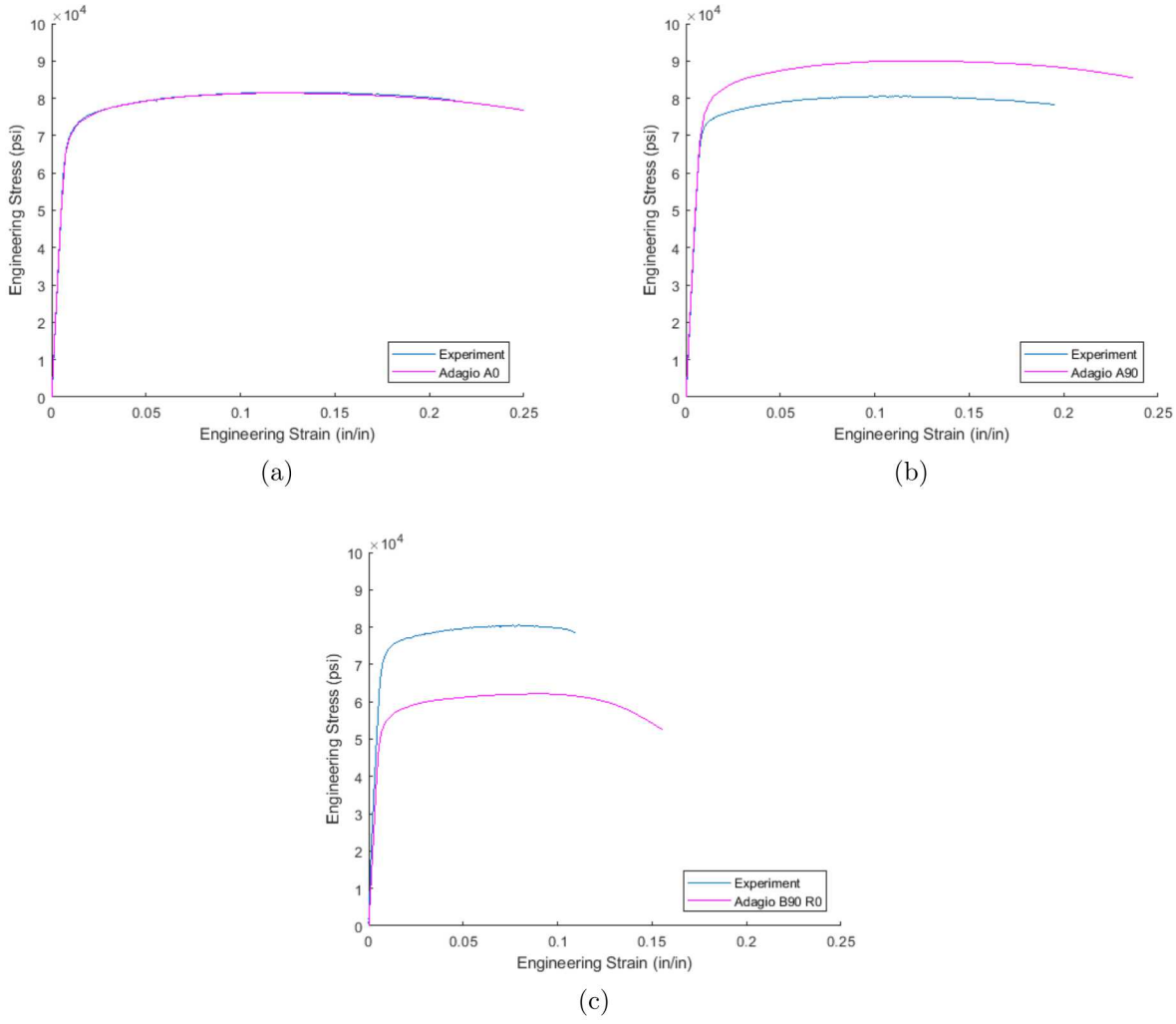

Figure 7: Comparison of the experimental and Hill model simulation stress-strain curves for the different material orientations of the uniform cross-section specimen in a uniaxial tension test. (a) A0 orientaton (b) A90 orientation and (c) B90 orientation.

The results in Figures 8a-8c show how Barlat model fits closer to the experimental data than Hill, demonstrating how Barlat can better model the responses of anisotropic materials. Thus it is recommended to use the Barlat model for more accurate results in anisotropic material studies. Figures 9a and 9b show the stress and strain at the ultimate point for several values of the flow stress weighting factor for the Hill model. The major trend seen in Figure 9a

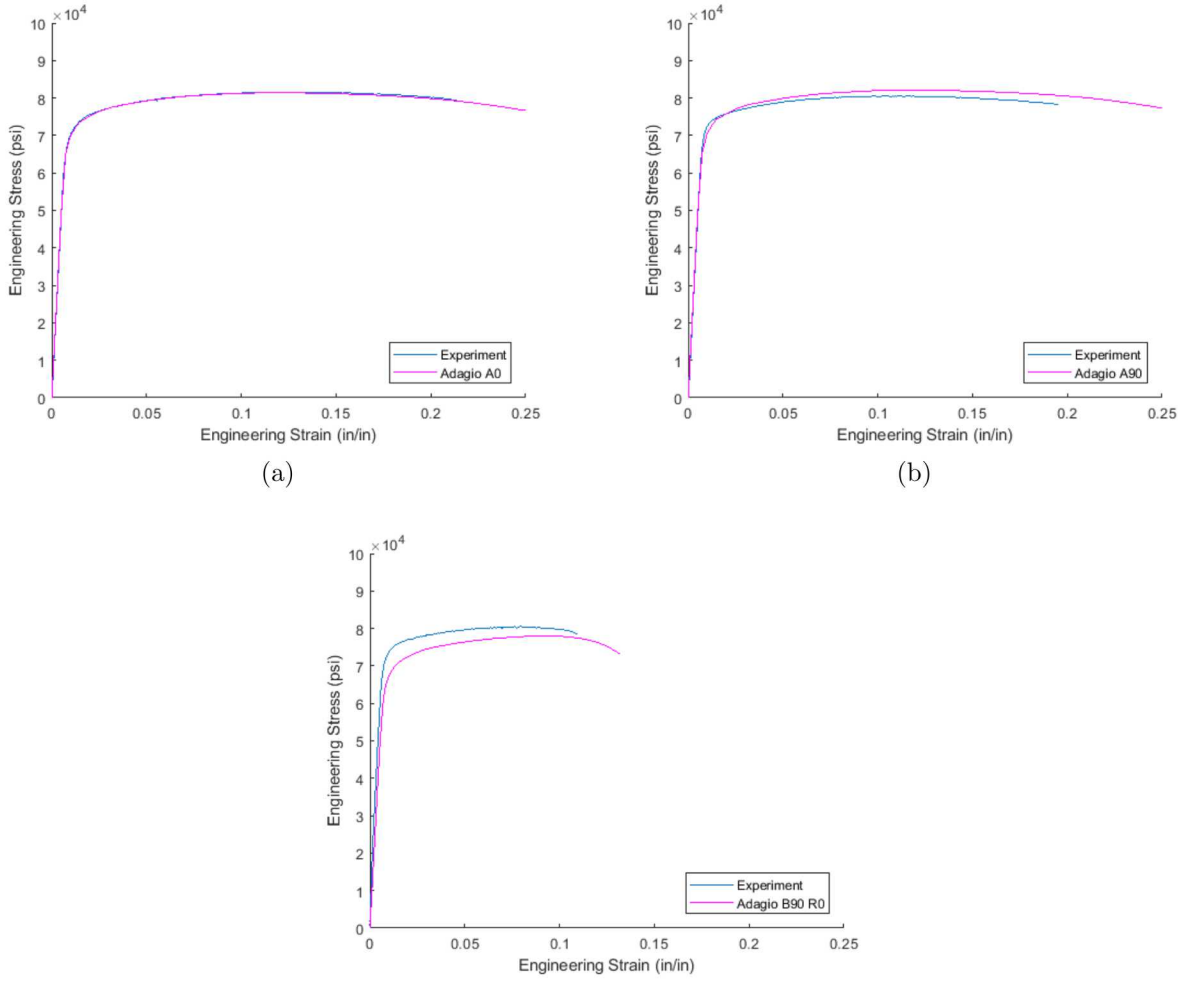

Figure 8: Comparison of the experimental and Barlat model simulation stress-strain curves for the different material orientations of the uniform cross-section specimen in a uniaxial tension test. (a) A0 orientaton (b) A90 orientation and (c) B90 orientation.

shows a decrease in the ultimate stress as weight increases. The strain value at ultimate does not vary much as the weight changes in Figure 9b except when w_σ= 15. These trends are also effected in the normalized plots in Figures 9c and 9d. Barlat shows the ultimate stresses converging in Figures 10a and 10c and little change in the strain values at ultimate among the calibrations in Figures 10b and 10d.

The results shown in Figures 9 and 10 show why the choices made by the analyst during calibration are important. The Hill model shows as great as a 10% difference in the ulitmate stress as the weight changes from 2 to 30. If weight 0 is inlcuded, where the flow stress is not considered in calibration, then the difference is 20%, showing the importance of considering both the flow stress and Lankford ratio in calibration. Some weights, such as weight 15, show more variance, as seen in Figures 9c and 9d, so it is recommended to calibrate with more

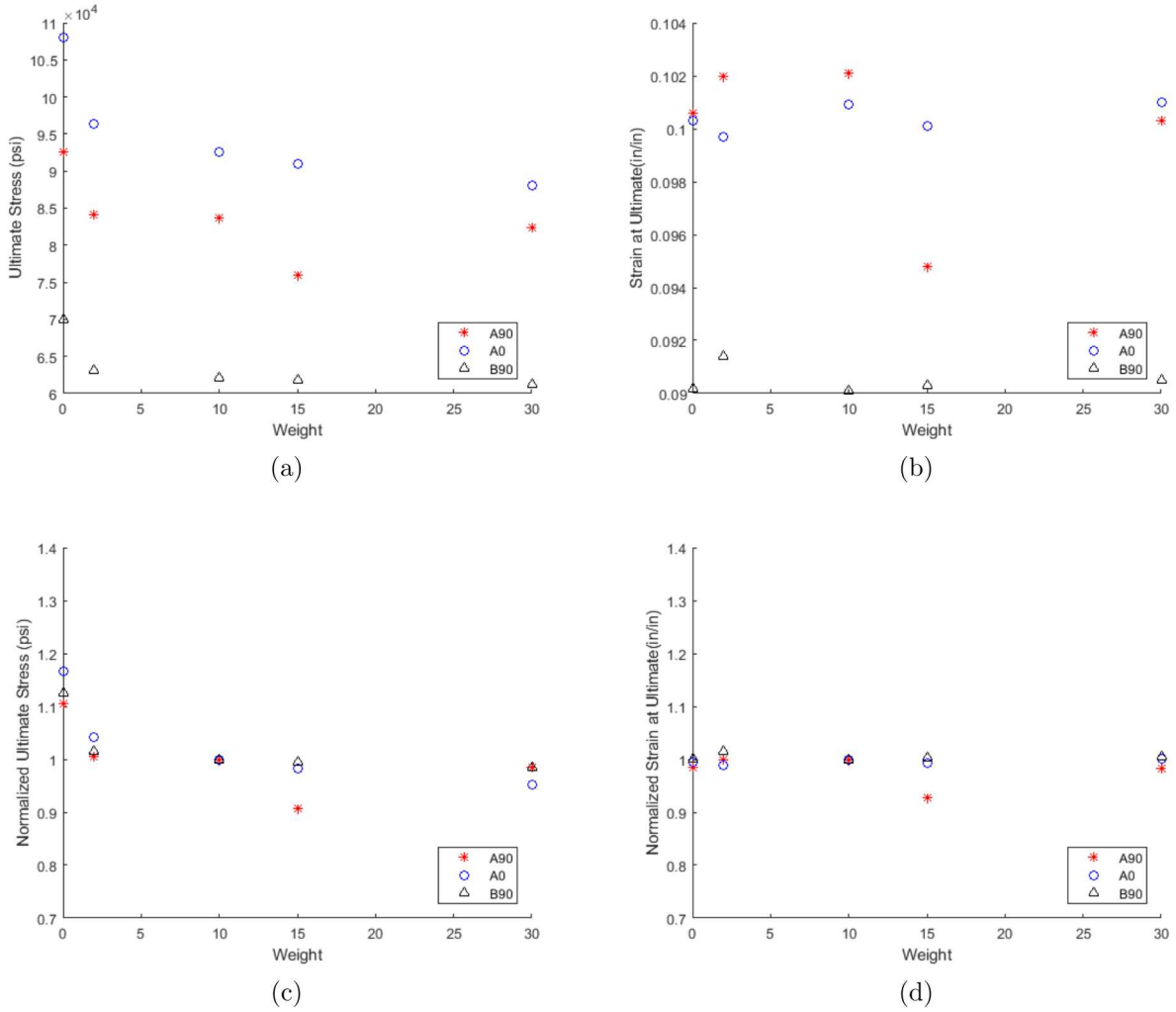

Figure 9: Comparison of the experimental and Hill simulation material response at the ultimate point. (a) Stress at the ultimate point (b) strain at the ultimate point and (c) normalized stress at the ultimate point and (d) normalized strain at the ultimate point.

than one weight to ensure the weight chosen does not have unusual variability compared with other weights.

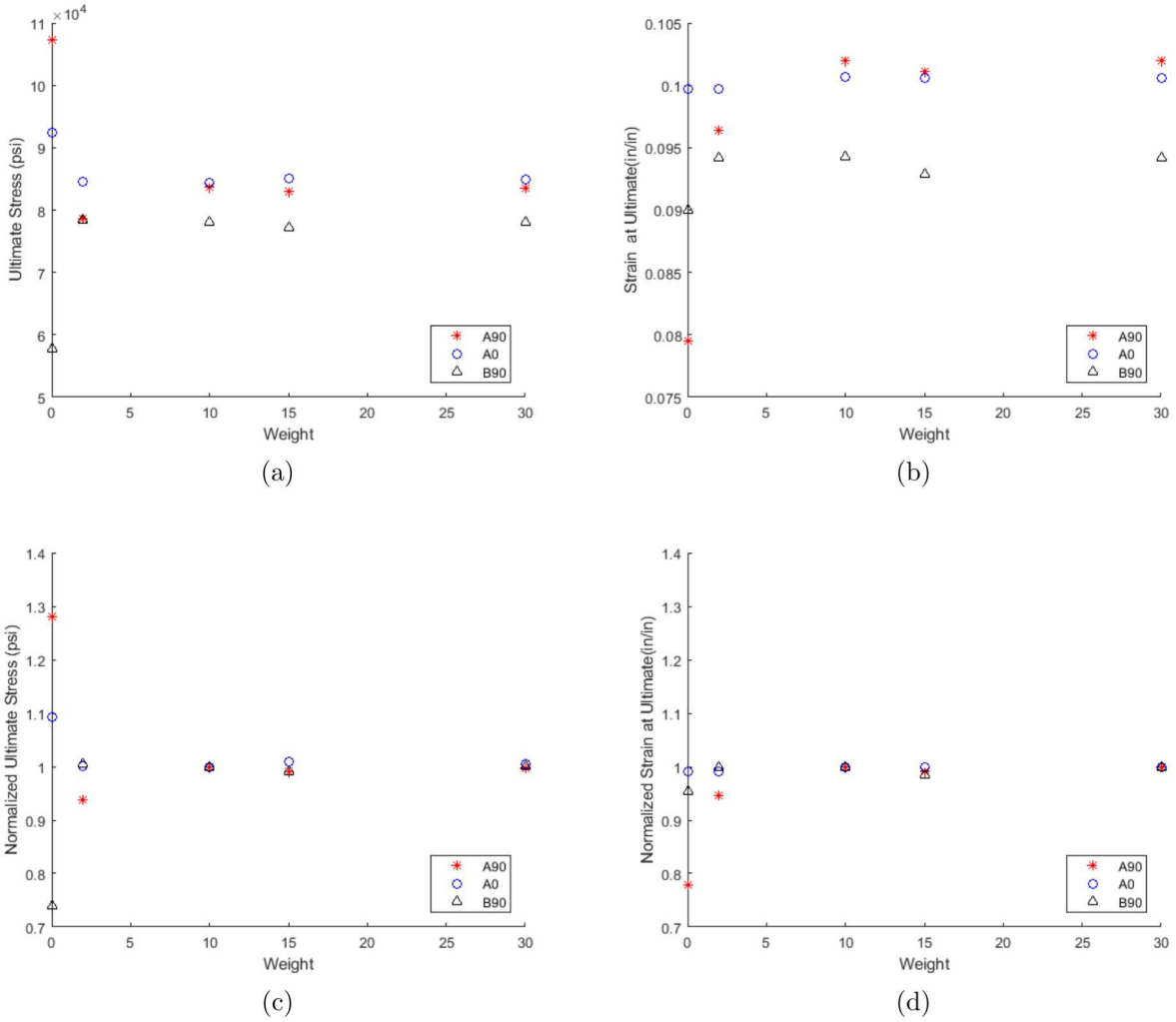

Figure 10: Comparison of the experimental and Barlat simulation material response at the ultimate point. (a) Stress at the ultimate point (b) strain at the ultimate point (c) normalized stress at the ultimate point and (d) normalized strain at the ultimate point.

2.3 Model Validation Specimen

Procedure

In addition to the the uniform cross-section specimens, there were four material orientations tested with rectangular specimens designed with a hole in the middle to induce multiaxial states of stress, as shown in Figure 11. Specimens A, B, and C had their long sides along the axis of the extrusion. The specimen orientations are as follows: specimen A was in the axial-through-thickness plane, specimen B was in the axial-circumferential plane, specimen C was rotated 45° to the through-thickness direction, and specimen D was in the axial-circumferential plane but its long side was in the circumferential direction. Figure 12 shows these orientations.

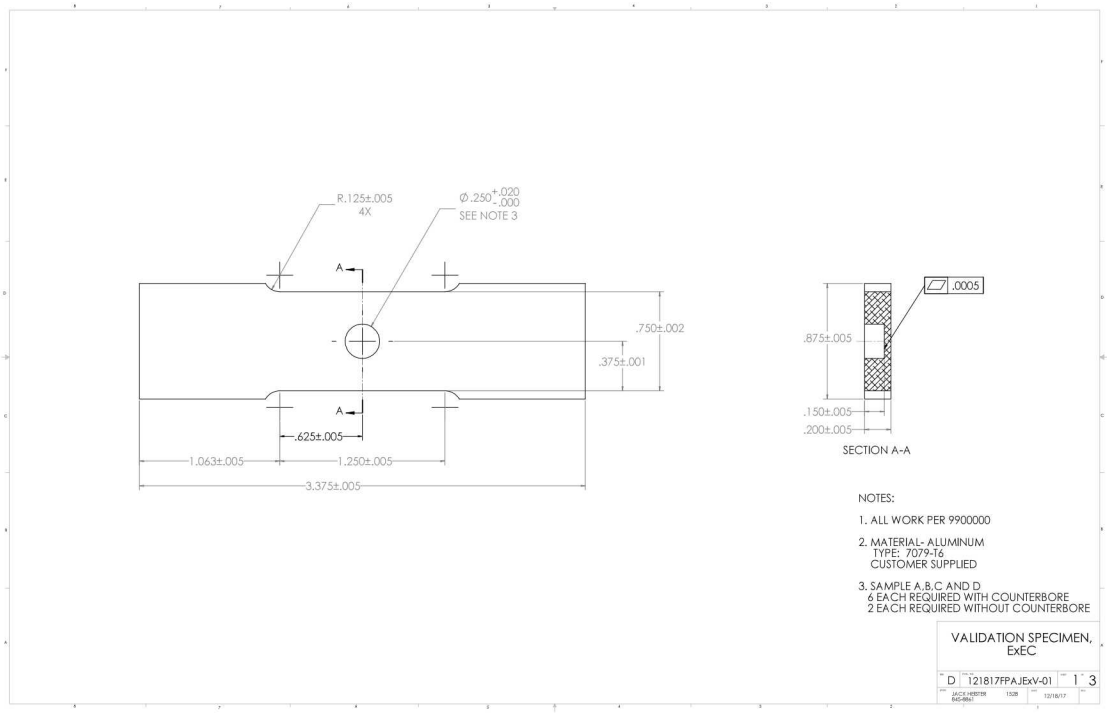

Figure 11: Validation specimen design.

The Barlat model was used to simulate these specimens with the parameters obtained with a flow stress weighting factor of 10 and a Lankford ratio weighting factor of unity in Sierra/SM. Then the load-displacement data for all experimental tests and simulations were compared.

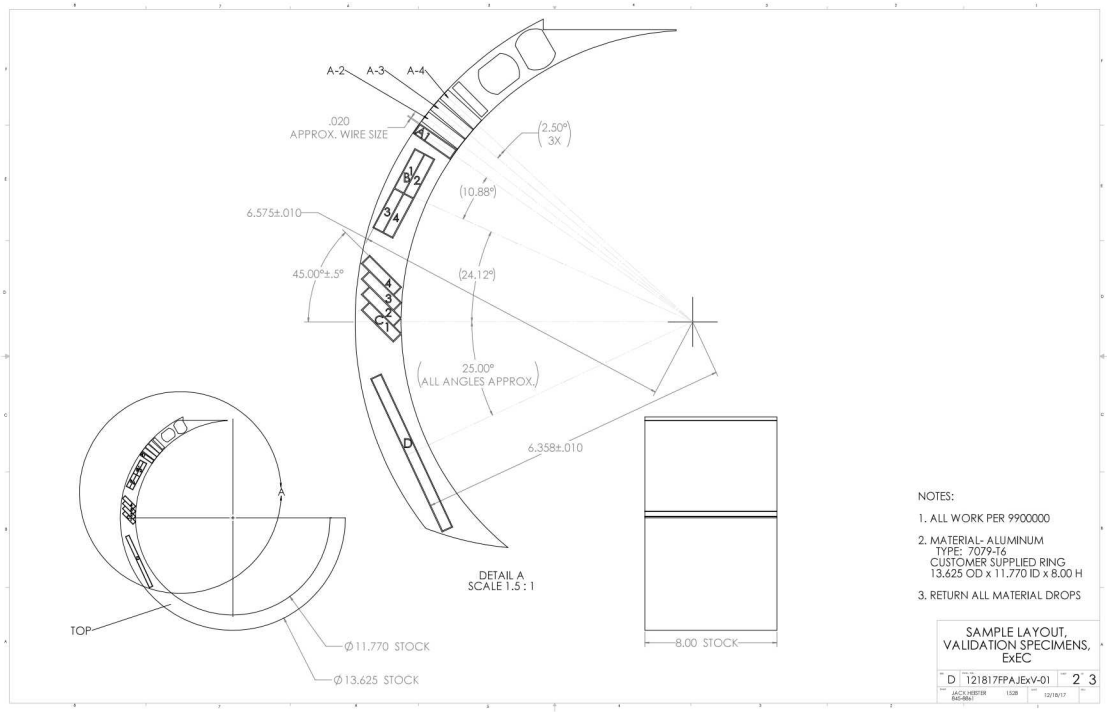

Figure 12: The four orientations of the validation specimens.

Strain maps from Digital Image Correlation (DIC) images generated from the experiments were compared with equivalent strain maps calculated from the finite element simulations.

Results

The simulation data in Figures 13a-13d overpredicted the load in the order of 3-5% in all cases. There was not much difference between the Barlat and isotropic models among the different orientations. However, the shape of the load-displacement curves from the experiments changed depending on the orientation as seen in Figure 14 which compares all four orientations. The Barlat model predictions showed less sensitivity to the specimen orientation.

The effects of anisotropy in the material are more pronounced in the strain maps. When the two normal strains, transverse to the specimen axis and along the specimen axis, and shear strain were mapped on the smooth sufrace of the specimen, the strain fields generally matched between the experiments and Sierra/SM simulations, both in color scheme and the

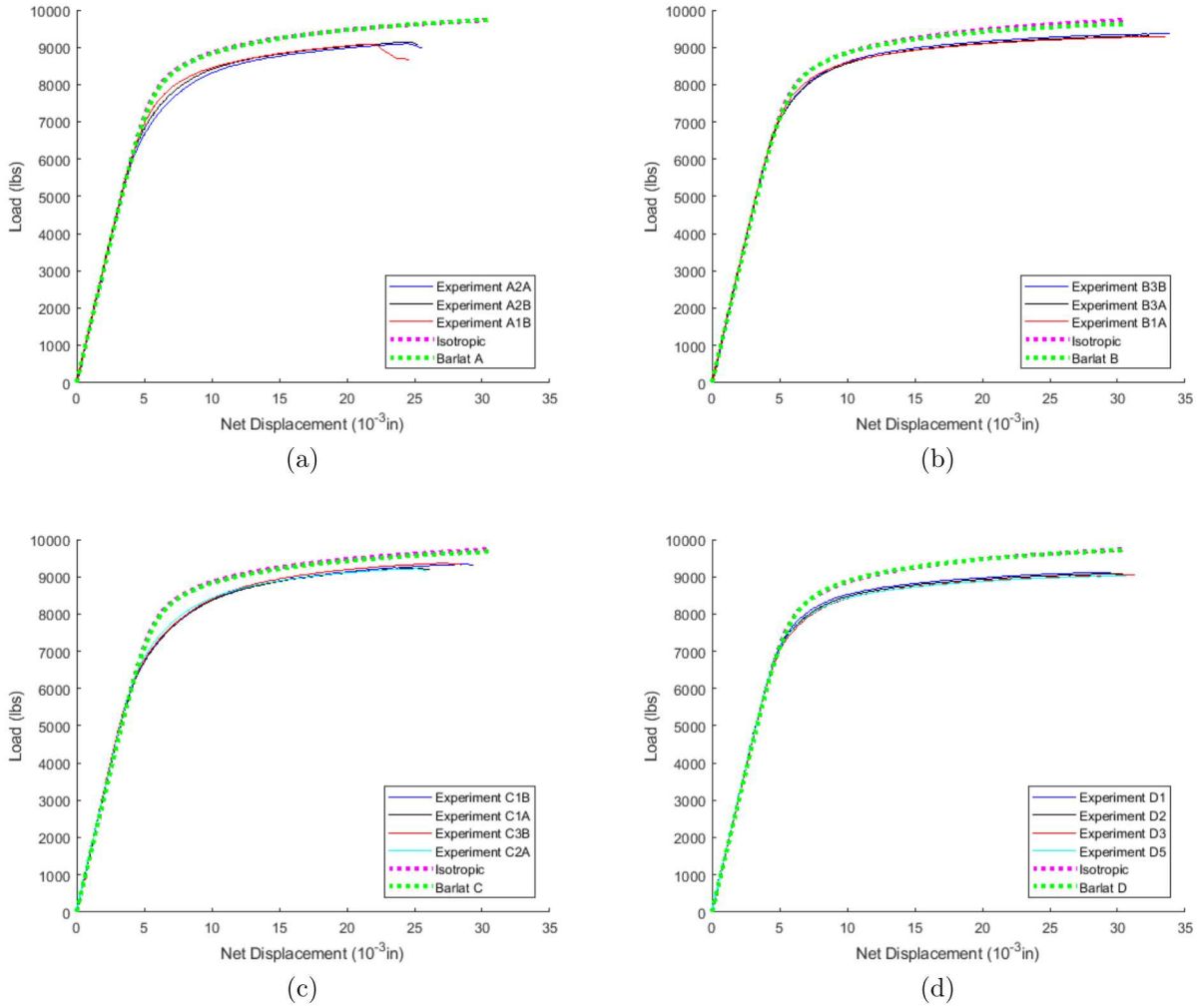

Figure 13: Comparing the experimental and simulation load-displacement curves for the different material orientations of the validation specimen. (a) A orientaton (b) B orientation (c) C orientation and (d) D orientation.

shape of the strain fields. Figures 15, 16, 17, and 18, show comparisons of the strain fields between measurements and predictions for the A, B, C, and D orientations, respectively at a net displacement of 0.0175 inches. Figure 19 shows an isotropic material response for comparison to the anisoptropic responses in A, B, C, and D. The isotropic results are insensitive to orientation and therefore would not accurately represent all the orientations like the Barlat model results. This study helps validate the Barlat model's ability to simulate the material response of an anisotropic material.

The anisotropy among the specimens determines the shape of the load displacement curves and the strain fields, which the Barlat material model reasonably matched. This is helpful in demonstrating that the Barlat model has the potential to model the elastic-plastic response of metals more accurately than simpler models.

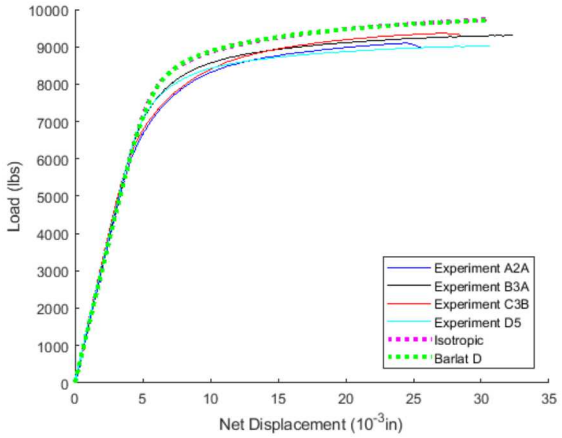

Figure 14: Load-displacement curves for all material orientations.

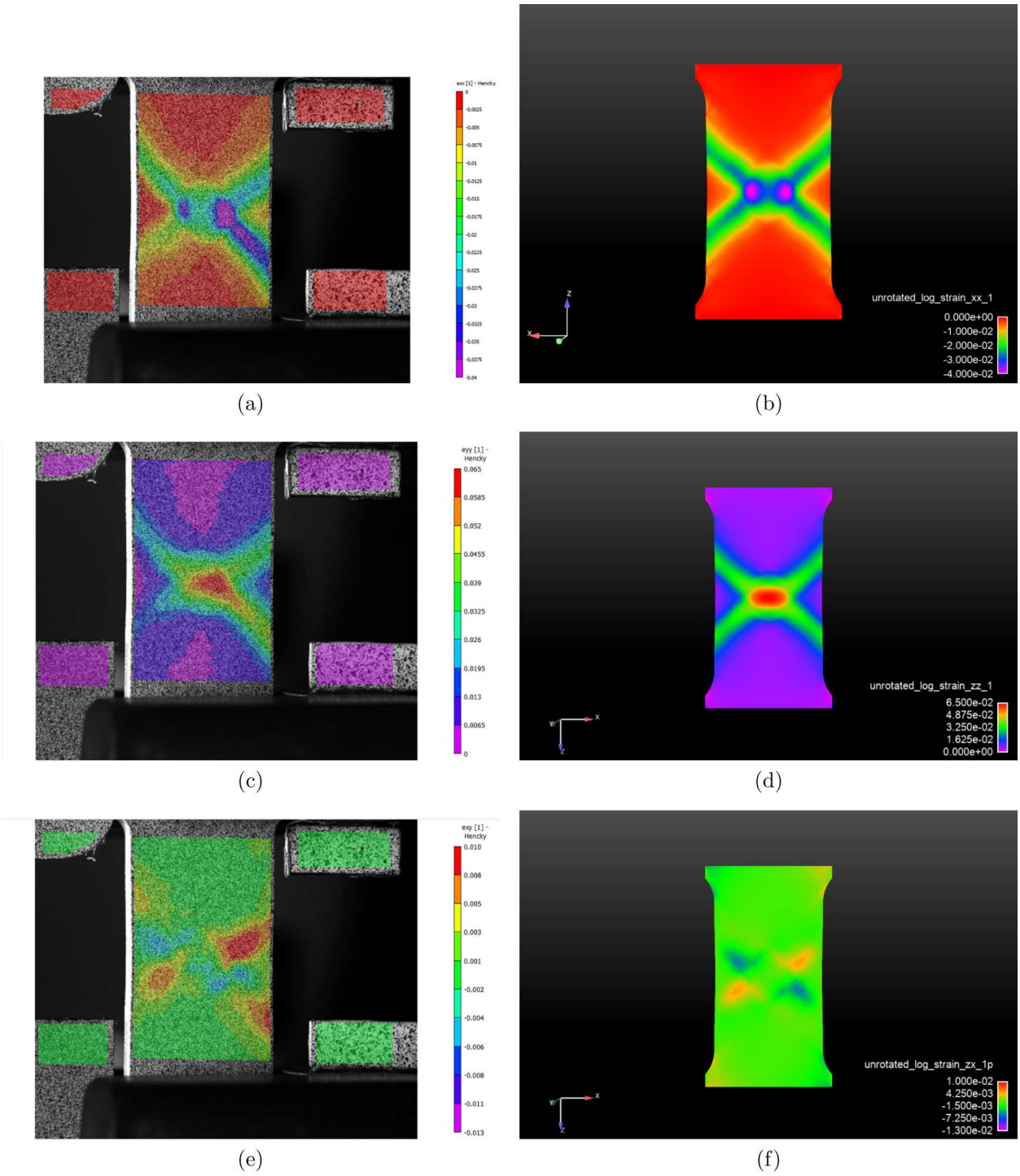

Figure 15: Comparison of experimental and Barlat simulation strain fields of the A specimens at a net displacement of 0.0175 inches. (a) Experimental transverse (b) Barlat simulation transverse (c) experimental axial (d) Barlat simulation axial (e) experimental shear and (f) Barlat simulation shear.

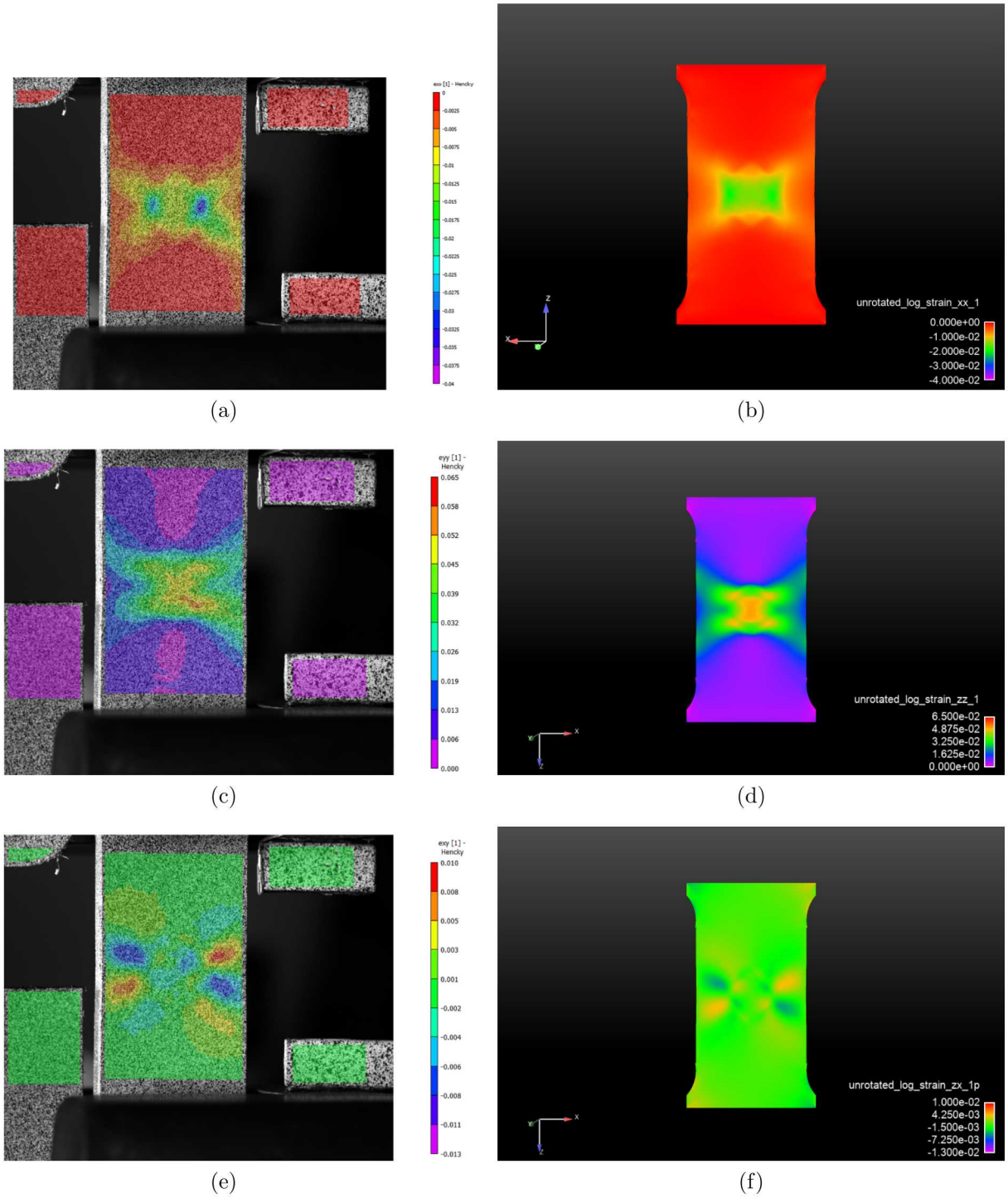

Figure 16: Comparison of experimental and Barlat simulation strain fields of the B specimens at a net displacement of 0.0175 inches. (a) Experimental transverse (b) Barlat simulation transverse (c) experimental axial (d) Barlat simulation axial (e) experimental shear and (f) Barlat simulation shear.

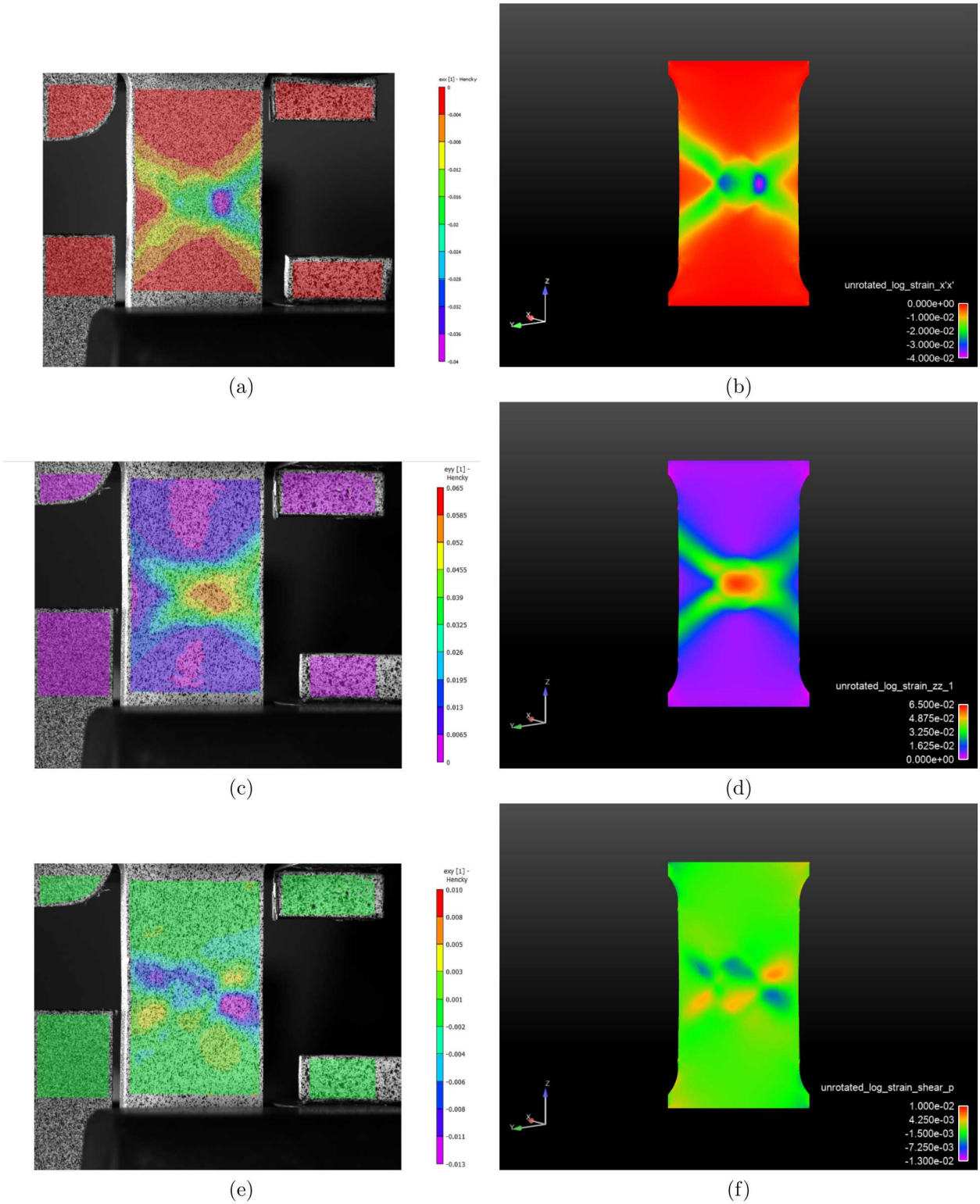

Figure 17: Comparison of experimental and Barlat simulation strain fields of the C specimens at a net displacement of 0.0175 inches. (a) Experimental tansverse (b) Barlat simulation transverse (c) experimental axial (d) Barlat simulation axial (e) experimental shear and (f) Barlat simulation shear.

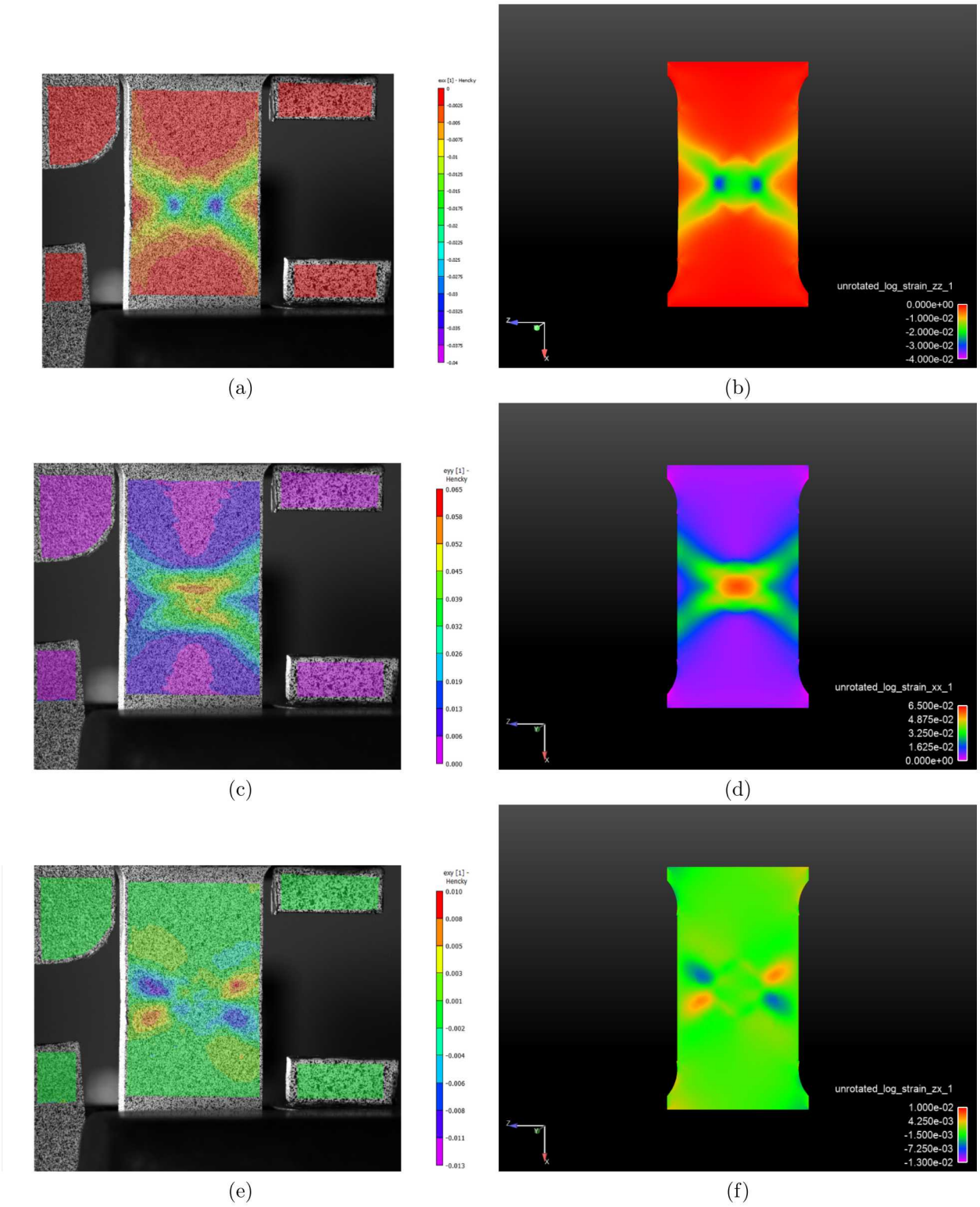

Figure 18: Comparison of experimental and Barlat simulation strain fields of the D specimens at a net displacement of 0.0175 inches. (a) Experimental transverse (b) Barlat simulation transverse (c) experimental axial (d) Barlat simulation axial (e) experimental shear and (f) Barlat simulation shear.

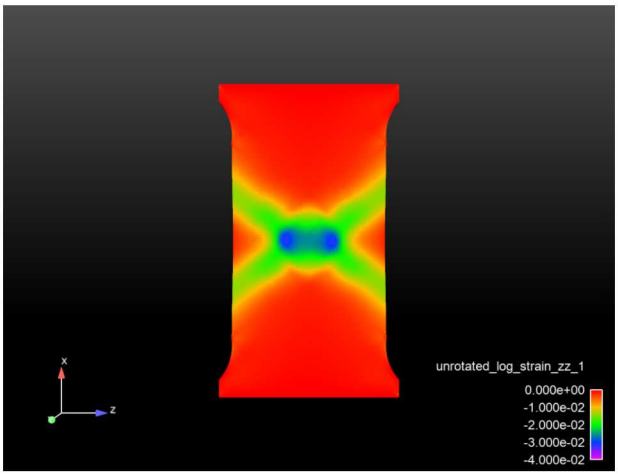

(a)

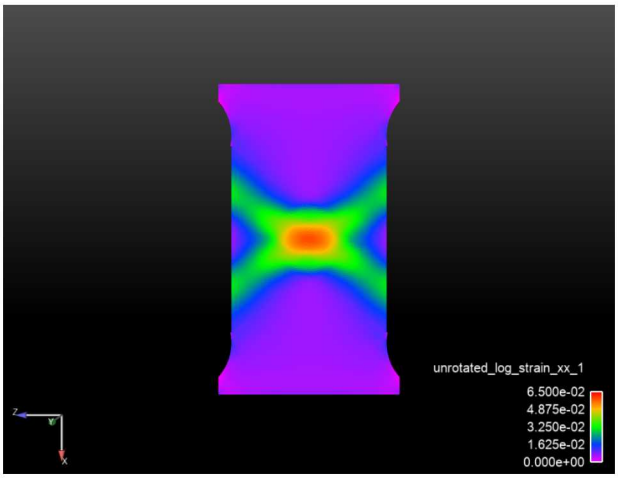

(b)

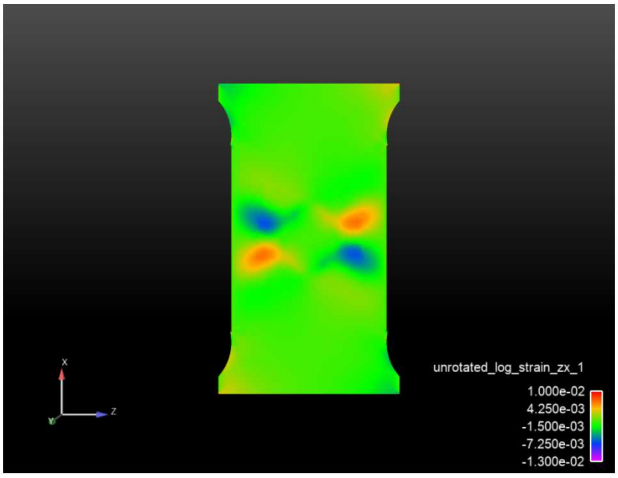

(c)

Figure 19: Isotropic simulation strain field results at a net displacement of 0.0175 inches. (a) Isotropic transverse (b) isotropic axial and (c) isotropic shear.

3 Conclusions

While changing the calibrations of the Hill and Barlat elastic-plastic material models, the sensitivity of the models' parameters could be evaluated. Some parameters were more sensitive to changes in the calibration weights than others. The changes in calibration parameters made a difference in the calculated material response, such as the stress-strain curve in uniaxial tension test simulations. The results presented here demonstrated how important the choice of model parameters is when simulating a material's behavior. For the cases in this study, when using the Barlat model a flow stress weight of 5 and Lankford weight of 1 is recommended based on the calibration error trends for each model. For the Hill model, a flow stress weight between 1 and 15 with a Lankford weight of 1 is recommended.

The effects of anisotropy can be demonstrated with the shape of the load-displacement curves and the strain fields along with the differences among values of the ultimate stress and Lankford ratios of different material orientations. The Barlat model was able to achieve a closer fit to the anisotropy effects observed in the tests when compared to the Hill model. This could be expected since it has three times more parameters to model anisotropy than the Hill model. Furthermore, the results of the Barlat model matched the experimental anisotropic material response in the strain fields for a speicimen geometry with multiaxial stresses, thus validating the ability of the Barlat model to simulate with more complex geometries with anisotropy.

For further studies, calibrating models with more than one weight is recommended to ensure a weight with unusual variability is not chosen. Additionally, analysts should avoid choosing extreme weighting factor values. The flow stress and Lankford ratio are necessary when modeling the effects of anisotropy on yield, so calibration procedures should not neglect one or the other.

References

Barlat, F., Aretz, H., Yoon, J.W., Karabin, M.E., Brem, J.C. and Dick, R.E. (2005), Linear transformation-based anisotropic yield function, *International Journal of Plasticity*, **2**1, pp. 1009-1039.

Corona, E. and Kramer, S. (2017), Experimentally enhanced computation (ExEC): Traditional calibration of anisotropic yield functions. SAND2017-9518R.

Hill, R. (1948), A theory of the yielding and plastic flow of anisotropic metals, *Proceedings of the Royal Society of London, Series A, Mathematical and Physical Sciences*, **193**, pp. 281-297.

Acknowledgements

This project would not have been possible without the guidance of Edmundo Corona, Brian Lester, Ben Reedlunn, and the testing and data processing of Amanda Jones.

Sandia National Laboratories is a multimission laboratory managed and operated by National Technology & Engineering Solutions of Sandia, LLC, a wholly owned subsidary of Honeywell International Inc., for the U.S. Department of Energy's National Nuclear Security Administraion under contract DE-NA0003525.

External Distribution:

Olivia McIntee, CU Boulder

Internal Distribution:

E. Jones	1512
A. Jones	1528
S. Kramer	1528
J. Redmond	1550
E. Corona	1554
E. Fang	1554
B. Lester	1554
B. Reedlunn	1554
W. Sherzinger	1554
A. Brown	8259
K. Karlson	8259